ARTICLE IN PRESS

Available online at www.sciencedirect.com
SCIENCE DIRECT®

Molecular Phylogenetics and Evolution xxx (2005) xxx–xxx

MOLECULAR PHYLOGENETICS AND EVOLUTION

www.elsevier.com/locate/ympev

Complex evolutionary history of a Neotropical lowland forest bird (*Lepidothrix coronata*) and its implications for historical hypotheses of the origin of Neotropical avian diversity

Z.A. Cheviron [a,*], Shannon J. Hackett [b], Angelo P. Capparella [a]

[a] *Department of Biological Sciences, Illinois State University, Normal, IL 61790, USA*
[b] *Department of Zoology, Field Museum of Natural History, 1400 South Lake Shore Dr., Chicago, IL 60605, USA*

Received 4 October 2004; revised 11 January 2005

Abstract

Here we apply a combination of phylogeographic and historical demographic analyses to the study of mtDNA sequence variation within the Blue-crowned Manakin (*Lepidothrix coronata*), a widespread Neotropical bird. A high degree of phylogeographic structure allowed us to demonstrate that several vicariant events, including Andean uplift, the formation of riverine barriers, and climatically induced vegetational shifts, as well as a non-vicariant process, range expansion, have all acted, at varying spatial and temporal scales, to influence genetic structure within *L. coronata*, suggesting that current historical hypotheses of the origin of Neotropical avian diversity that focus on single vicariant mechanisms may be overly simplistic. Our data also support an origin (>2 mybp) that is substantially older than the late Pleistocene for the genetic structure within this species and indicate that phylogeographic patterns within the species are not concordant with plumage-based subspecific taxonomy. These data add to a growing body of evidence suggesting that the origin of several Neotropical avian species may have occurred in the mid-Pliocene, thus, geological arguments surrounding putative Pleistocene vicariant events, while interesting in their own right, may have little relevance to Neotropical avian diversification at the species level.

Keywords: Amazonia; Historical demography; *Lepidothrix*; Neotropics; Nested clade analysis; Phylogeography; Refugia; Vicariant events

1. Introduction

The Neotropical rainforests of Central and South America harbor the highest level of avian biodiversity in the world (Haffer, 1990), and the processes that have promoted this high degree of diversification have intrigued evolutionary biologists for over a century (Chapman, 1917, 1926; Moritz et al., 2000; Wallace, 1889). Historically, these questions have been approached from a biogeographic perspective, and this work has led to the formulation of a number of hypotheses that attribute Neotropical avian diversity to historical factors (but see Endler, 1982). These historical hypotheses generally evoke vicariant mechanisms, such as Andean uplift (Chapman, 1917), Pleistocene forest refugia (Haffer, 1969), riverine barriers (Sick, 1967), and marine transgressions (Nores, 1999) (reviewed in Haffer, 1997). These hypotheses have undoubtedly been influential in stimulating evolutionary studies in the region, but their explanatory power is limited because they are based almost entirely on distribution data of morphologically distinct taxa, which is problematic for two reasons. First, distribution data do not incorporate the phylogenetic component of the distributions of taxa (Brooks and van Veller, 2003), which is often of the

* Corresponding author. Present address: Museum of Natural Science and Department of Biological Sciences, Louisiana State University, Baton Rouge, LA 70803, USA. Fax: +1 225 578 3075.
E-mail address: zchevi1@lsu.edu (Z.A. Cheviron).

1055-7903/$ - see front matter © 2005 Elsevier Inc. All rights reserved.
doi:10.1016/j.ympev.2005.01.015

greatest interest in evolutionary studies; and second, recent genetic surveys have shown that morphologically defined taxa may misrepresent patterns of genetic diversity in Neotropical birds (Marks et al., 2002; Moritz et al., 2000; Zink, 2004). These problems can be overcome by utilizing a phylogeographic approach (Avise, 2000), but such studies of Neotropical birds are few (but see Aleixo, 2004; Bates et al., 2003; Brumfield and Capparella, 1996; Brumfield et al., 2001; Marks et al., 2002).

Classic phylogeographic approaches generally involve overlying a phylogeny onto geography (sampling sites) and then examining the degree of congruence between clade distributions and ecogeographic barriers. Although informative, this approach alone cannot be used to distinguish among historical events and contemporary processes because identical phylogeographic patterns may be produced by unrelated processes (Hoffman and Blouin, 2004; Templeton et al., 1995). Analytical advances have led to the development of methodologies for inferring the causes of divergence among taxa and reconstructing the recent demographic history of populations. Nested clade phylogeographical analysis (NCPA—Templeton, 2004) uses a parsimony-based haplotype network to define a series of nested sets (clades) following the nesting rules of Templeton et al. (1987); Templeton et al. (1992), and Clement et al. (2000). This nesting design is then combined with haplotype sampling locations, and permutation analyses are used to statistically test for phylogeographic associations. Once significant phylogeographic structure is detected, NCPA uses the geographical distances within and among nested clades to make inferences about the causal mechanisms of the observed statistically significant phylogeographic associations. With adequate geographic and genetic sampling, NCPA can be used to begin to discriminate among associations that are due to recurring but restricted gene flow and those that are due to historical events such as past fragmentation, colonization, or range expansion (Durand et al., 1999; Templeton, 1998, 2004). Phylogeographic inferences can be corroborated by estimates of historical demography; several techniques have been developed to statistically test for historical changes in population size (reviewed in Fu, 1997). The application of NCPA and historical demographic analyses, in conjunction with classical phylogeography, allows for the reconstruction of the evolutionary histories of taxa in unprecedented detail (Hoffman and Blouin, 2004). As a result, evolutionary biologists are now in a position to reevaluate their understanding of Neotropical avian evolution in light of these theoretical and analytical advances.

1.1. Study taxon

The Blue-crowned Manakin (*Lepidothrix coronata*) is a widespread Neotropical passerine, occurring throughout much of western Amazonia, the Chocó region of western Colombia and Ecuador, and southern Central America. It is a relatively common frugivore, restricted to the understory of mature unflooded *terra firme* forest (Ridgley and Tudor, 1994). *L. coronata* exhibits a substantial amount of geographic variation in male plumage across its range. The eight described subspecies can be divided into two subspecies groups, the *coronata* subspecies group (*coronata*, *carbonata*, *caquetae*, *minuscula*, and *velutina*) with males of predominately black plumage and the *exquisita* subspecies group (*exquisita*, *caelestipileata*, and *regalis*) with males of predominately green plumage (Traylor, 1979). Subspecies of the *coronata* group occur in Central America (Costa Rica and Panama), west of the Andes in Colombia and northwestern Ecuador, and east of the Andes in western Amazonia as far south as the northwestern portion of the department of Cuzco in Peru and as far east as central Venezuela. Subspecies of the *exquisita* group occur in central Peru, south to north-central Bolivia and as far east as southwestern Amazonas, Brazil. Throughout much of Amazonia the black form occurs in the northern portion of the range and is replaced to the south by the green form. A zone of intergradation between the two forms occurs in east-central Peru and western Brazil (Haffer, 1970).

The Blue-crowned Manakin has figured prominently in the development of two Neotropical historical hypotheses. Plumage variation within the species was instrumental in the early development of the refugia hypothesis (Haffer, 1970, 1974). The zone of intergradation between the black and green plumaged subspecies groups in east-central Peru and western Brazil has been hypothesized to be a suture zone and most consistent with the refugia hypothesis because it appears to occur in continuous forest away from any contemporary barrier (Haffer, 1970, 1974). Capparella (1988, 1991), however, demonstrated substantial genetic structure among morphologically identical populations on opposite sides of the Amazon and Napo rivers, a result consistent with the riverine barrier hypothesis (Moritz et al., 2000; Sick, 1967). Its widespread range, high degree of geographic variation, restriction to understory of *terra firme* forest, and historical relevance make *L. coronata* an ideal candidate for a study of this nature.

We examined mtDNA sequence variation within the Blue-crowned Manakin to address several questions regarding the genetic structure and evolutionary history of the species. First, does phylogeographic structure correspond to subspecific taxonomy; that is, do patterns of plumage variation accurately reflect patterns of genetic diversity within the species? Second, what proportion of the genetic breaks within the species correspond to contemporary ecogeographic barriers, and do these barriers represent primary or secondary barriers to gene flow? Here we define a primary barrier as a barrier that was

the cause of divergence between clades. A secondary barrier is defined as a barrier that limits the current distributions of two clades, but was not the initial cause of their divergence. And finally, if genetic population structure occurs in the absence of a barrier, are phylogeographic and historical demographic patterns consistent with any previously proposed hypothesis of the origin of Neotropical biodiversity?

2. Materials and methods

2.1. Taxon sampling

Sixty-four individuals from 29 collecting localities within the range of *L. coronata* were sampled (Appendix A and Fig. 1). Sample sites were chosen to maximize the geographic scope of the sampling design. One to six individuals from each site were sampled (Appendix A). All tissue samples used in this study were obtained on loan from the following institutions (alphabetical by institution): Academy of Natural Sciences—Philadelphia (ANSP), American Museum of Natural History (AMNH), Field Museum of Natural History (FMNH), Kansas University Museum of Natural History (KUMNH), and Louisiana State University Museum of Natural Science (LSUMNS). Recent studies of mtDNA sequence variation has placed a clade composed of *L. coeruleocapilla*, *L. isidorei*, *L. nattereri*, and *L. iris* as sister to *L. coronata* (Hackett unpubl. data). Thus, one individual of both *L. coeruleocapilla* and *L. iris*, along with one individual of the more distantly related *L. serena*, were included as outgroups.

2.2. Amplification and sequencing

Total genomic DNA was extracted from approximately 10 mg of muscle tissue using a QIAamp DNA extraction kit (Qiagen). Fragments of the mitochondrial cytochrome *b* and ND2 genes and the entire mitochondrial ND3 gene were amplified via polymerase chain reaction (PCR) using published mtDNA primers [cytochrome *b*, L14841, and H16065 (Kocher et al., 1989); ND2, H5578, and L5215 (Hackett, 1996); ND3, H11151, and L10755 (Chesser, 1999)]. All amplification reactions were performed in 50 μl volumes using an MJ Research Model PTC-200 Peltier thermal cycler under the following conditions: (1) an initial denaturing step at 94 °C for 7 min; (2) 35 cycles of the following: 1 min at 92 °C, 1 min at 50 °C, and 1 min at 72 °C; and (3) a 7 min extension step at 72 °C. Following PCR, correct fragment size and the presence of a single amplification product was confirmed via electrophoresis run on an agarose gel. Amplified mtDNA was purified using a Geneclean II kit (Bio 101). Cleaned double-stranded PCR product was cycle-sequenced with dye terminators (ABI Big Dye Terminator Cycle Sequencing Kit with AmpliTaq DNA Polymerase, FS; Applied Biosystems) and the aforementioned primers for 25 cycles under the following conditions: 96 °C for 10 s, 50 °C for 15 s, and 60 °C for 4 min. Following ethanol precipitation, sequencing products were resuspended in Template Suppression Reagent (Applied

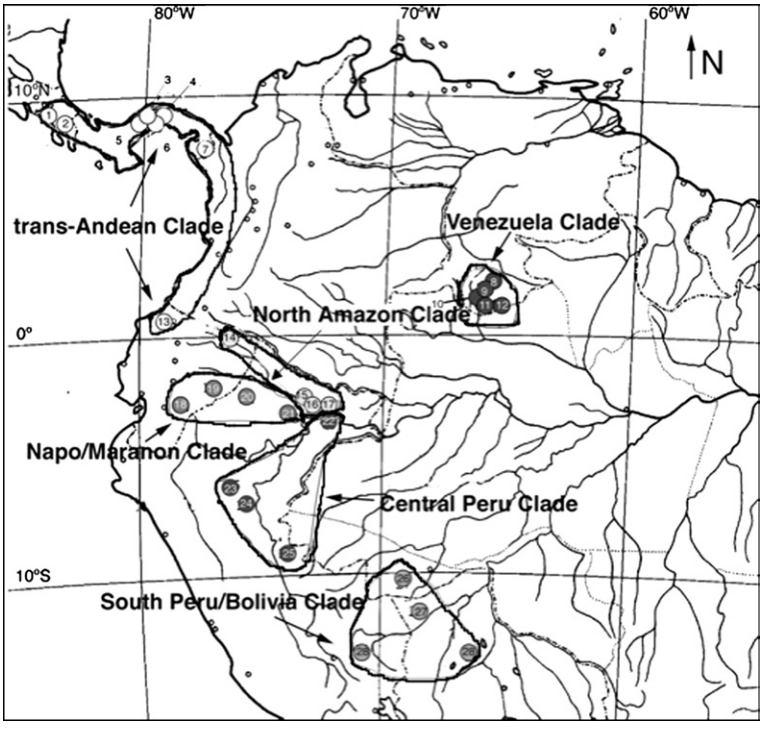

Fig. 1. Distributions of haplotype clades and collection localities for tissue samples. Site numbers correspond to Appendix A.

Biosystems) and visualized using an ABI Prism 310 automated sequencer (PE Applied Biosystems).

2.3. Data exploration

DNA sequences from both strands were aligned using the computer program Sequencher 4.1 (Gene Codes Corporation). Aligned sequences were compared and any differences between them were resolved by eye. Several precautions were taken to ensure that sequences were mitochondrial in origin. All electropherograms were closely examined for the presence of double peaks in both strands. Sequences were aligned with *Gallus gallus domesticus* (chicken) mitochondrial sequence (Desjardins and Morais, 1990), allowing protein-coding regions to be translated to amino acid sequence and examined for the presence of insertions, deletions, and stop codons that would render protein-coding regions non-functional. All sequences were expected to exhibit substitution patterns typical of mitochondrial genes (i.e., have high transition to transversion ratios). Partition-homogeneity tests were performed to ensure similar phylogenetic signal among all three gene fragments. Finally, genetic distance matrices were examined for any obviously different sequences. Similar measures have been used to check for the presence of nuclear pseudogenes in other avian molecular phylogenetic studies (e.g. Aleixo, 2002; Bates et al., 1999; Marks et al., 2002; Sorenson and Quinn, 1998).

Four partition-homogeneity tests were performed to assess congruence among data partitions. Each of these tests was performed using 100 replicates and only parsimony informative sites. First, three pair-wise comparisons of the protein-coding regions of each gene were performed. Second, all three codon positions of protein-coding regions were compared to test for evidence of saturation at the third codon position. Because there was no significant difference in phylogenetic signal among the individual genes, all fragments were analyzed together as a combined data set in all subsequent analyses.

2.4. Phylogenetic analyses

Phylogenetic analysis of DNA sequence data was performed using maximum-parsimony (MP) and maximum likelihood (ML) methods with the computer program PAUP*4.0b10 (Swofford, 1999) and Bayesian methods using the program MrBayes 3.0b4 (Hulsenbeck and Ronquist, 2001). *Lepidothrix iris*, *L. coeruleocapilla*, and *L. serena* were designated as outgroups in all phylogenetic analyses. Due to limits in computational time, phylogenetic analyses were performed using only unique haplotypes (52 unique *L. coronata* haplotypes were recovered).

Maximum parsimony analysis was performed using the "heuristic search" procedure with the following options: TBR branch-swapping with 1 random taxon addition replicate. Support for nodes in the parsimony tree was assessed using 1000 bootstrap iterations. Maximum likelihood and Bayesian analyses were also used to reconstruct the phylogeny of *L. coronata* haplotype lineages. ModelTest (Posada and Crandall, 1998) was used to perform a hierarchical likelihood ratio test to select the model of molecular evolution for maximum likelihood analysis. An HKY + G model of evolution (Hasegawa et al., 1985) was selected as best fit ($-\ln L = 3704.0405$) with the following parameters: unequal base frequencies (A = 0.2966, C = 0.2835, G = 0.1264, and T = 0.2935), transition/transversion ratio = 3.9928, and variable sites following a Γ distribution ($\alpha = 0.2694$). Support for nodes in the likelihood tree was assessed using 100 bootstrap iterations.

Bayesian analysis was performed using the computer program MrBayes 3.0b4 (Hulsenbeck and Ronquist, 2001) assuming an HKY + G model of evolution [all parameters (unequal base frequencies, variable ti/tv ratio, and variable sites following a Gamma distribution) were estimated using MrBayes]. Four Markov chains were run simultaneously for 600,000 generations with one tree being sampled every 10 generations. The Markov chain required roughly 20,000 generations to reach convergent and stable likelihood values. Thus, trees sampled prior to 20,000 generations were discarded. The remaining 58,000 trees were used to construct a strict consensus tree in PAUP. Support for nodes in the Bayesian tree was assessed using posterior probabilities.

2.5. Estimating divergence times

A molecular clock was forced on the ML topology and the likelihood scores of the two topologies (with clock enforced and without) were compared using a χ^2 test (df = # haplotypes − 2 = 53). Since the two topologies did not differ significantly ($\chi^2 = 46.1$, $P > 0.5$), it was assumed that all lineages evolved in a clock-like manner. We corrected for ancestral polymorphism within lineages following Edwards (1997) and Zheng et al. (2003). Divergence times were calculated by applying a calibration of 0.008 substitutions per site per lineage per million years to corrected divergence values. This rate corresponds to an estimate of 1.6% sequence divergence per million years, a divergence rate that is based on cytochrome *b* sequence variation in Hawaiian honeycreepers (Aves: Drepanidinae) and potassium–argon estimates of ages of the Hawaiian islands (Fleischer et al., 1998).

2.6. Nested clade phylogeographical analysis

The probability of a parsimonious relationship among haplotypes was calculated using the computer program TCS 1.13 (Clement et al., 2000) which imple-

ments the procedures described by Templeton et al. (1992). Haplotypes differing by up to 14 mutational steps had >95% probability of being connected parsimoniously and TCS was used to construct minimum spanning networks for these haplotypes. These networks were then used to define a nesting scheme following the nesting rules described by Templeton et al. (1987) and Templeton and Sing (1993). GeoDis 2.0 (Posada et al., 2000) was used to calculate clade distance (D_c), nested clade distance (D_n), and comparisons of these measures among interior and tip clades using the nesting scheme defined using TCS, by first defining the geographic center of each clade resolved at each hierarchical level. Second, distance between individuals and clade center was calculated using great circle distances (km). Comparisons of these measures were calculated using 1000 random permutations of clades and/or haplotypes against sampling locality to statistically test the null hypothesis of no geographic association among haplotypes or clades at each nesting level. Significantly ($\alpha = 0.05$) large or small clade distances or interior-tip contrasts imply geographic association. The inference key given by Templeton (2004) was used to infer the process (restricted but recurring gene flow, isolation by distance, allopatric fragmentation, contiguous range expansion, or long-distance colonization) most consistent with the observed statistically significant pattern at those nesting levels.

Several authors have questioned the accuracy of the inferences made by NCPA (Knowles and Maddison, 2002; Masta et al., 2003). Templeton (2004) has recently addressed these criticisms by analyzing empirical data sets with strong a priori expectations using a revised inference key. For the process of allopatric fragmentation, NCPA recovered the expected pattern in 61 of 66 cases (92.4%). Of the five "incorrect" inferences, four failed to detect an expected fragmentation event, whereas an unexpected fragmentation event (false positive) was inferred only once. For range expansion, NCPA recovered the expected pattern in 57 of 85 cases (67%). Again, the majority of "incorrect" inferences (75%) resulted from a failure to detect the expected pattern rather than the inference of an unexpected pattern (false positive). Note that failure to detect an expected pattern can be the result of inadequate sampling; thus, this type of error is conservative. The low frequency of detected false positives for allopatric fragmentation (1.5%) and range expansion (8.2%) is a considerable improvement over an earlier version of the inference key which recovered false positives for allopatric fragmentation and range expansion in 8 of 66 cases (12.1%) and in 17 of 85 cases (20%), respectively. These results suggest that inferences of these processes using the revised inference key (Templeton, 2004) are robust. Templeton (2004) concludes that the high rate of false positives suggested by Knowles and Maddison (2002) and Masta et al. (2003) for NCPA is due to the combined effects of two factors: (1) problems associated with the simulated data sets used to test the accuracy of NCPA and (2) problems with the older version of the inference key. The latter has been addressed by alterations to the most recent version. Despite the controversy surrounding the analysis, NCPA has recently been applied to the examination of phylogeographic structure in a wide range of invertebrate (e.g., de Brito et al., 2002; Masta et al., 2003; Wilke and Pfenniger, 2002) and vertebrate (e.g., Bernatchez, 2001; Durand et al., 1999; Hoffman and Blouin, 2004; Nesbo et al., 1999; Pavlova et al., 2003; Sgariglia and Burns, 2003; Templeton et al., 1995) taxa in both terrestrial and aquatic systems.

2.7. Historical demographic analyses

Demographic expansion was inferred by calculating Fu's F_s and Romis-Onsins and Rozas (2002) R_2 using DnaSp 3.53 (Rozas and Rozas, 1999). When calculating these statistics, populations were defined as major haplotype clades recovered in the phylogenetic analyses. Significance was determined based on 1000 coalescent simulations under a model of constant population size using empirical sample sizes and estimates of $\Theta(=4N_e\mu)$. Mismatch distributions (Rogers, 1995) were also calculated to compare the demographic histories of *L. coronata* populations. Again, populations were defined as the major haplotype lineages resolved in the phylogenetic analyses. The frequency of pairs of randomly chosen individuals differing by a given number of nucleotide substitutions and expected frequencies under a model of rapid demographic expansion were calculated using DnaSp. These expected frequencies were then overlayed onto the observed frequencies. Smooth Poisson mismatch distributions are characteristic of rapid demographic expansion. Harpending's (1994) raggedness index was used to measure the smoothness of the observed distributions and significance of raggedness indices was calculated using 1000 coalescent simulations with empirical estimates of Θ and τ. We did not attempt to infer demographic expansion for deeper nodes because doing so would have required combining divergent lineages into larger clades, confounding these inferences of historical demography.

2.8. Nucleotide diversity

Levels of nucleotide diversity (π) were calculated within each collecting locality where more than one individual was sampled as well as within major haplotype clades (for the purpose of calculating divergence times). π was calculated using standard equations (Nei, 1987) in Arlequin 2.0 (Schneider et al., 2000). High levels of nucleotide diversity are often indicative of population ancestry (Hewitt, 1996, 2000; Zink et al., 2000). Thus, populations with high levels of nucleotide diversity were inferred to be older than less diverse populations.

3. Results

3.1. Informative variation

A total of 1067 bp was sequenced for 61 *L. coronata* individuals and three outgroup taxa. Four tissue samples (ANSP 2490, ANSP 1408, ANSP 2140, and ANSP 5859) were badly decomposed making it impossible to obtain sequence data for the cytochrome *b* fragment. A total of 760 bp of the mitochondrial ND2 and ND3 genes were sequenced for these four individuals. All sequence data have been deposited in GenBank (Accession Nos. AY882069–AY882265).

For the ND2 fragment, 79 of 362 (21.8%) sites were variable. Of these variable sites, 47 (59.4%) were parsimony informative. As is typical of protein-coding genes, the vast majority (69.2%) of variable sites and 80.8% of parsimony informative sites occurred at the third codon position. Of the 398 bp of ND3 sequenced, 68 (17.1%) sites were variable, with 38 (55.9%) variable sites being parsimony informative. Sixty-seven percent of the variable sites and 71% of the parsimony informative sites occurred at the third codon position. For the cytochrome *b* fragment, 81 of 307 (26.4%) sites were variable. Of the 81 variable sites, 44 (54.3%) were parsimony informative. Again, the vast majority (71.6%) of variable sites and parsimony informative sites (93.2%) occurred at the third codon position. All three gene fragments exhibited base compositional biases typical of avian mitochondrial genes (Joseph et al., 2002) with each fragment being deficient in guanine (ND2—12.0%, ND3—12.1%, and cytochrome *b*—15.3%), especially at the third codon position (ND2—6.5%, ND3—1.5%, and cytochrome *b*—3.5%).

Levels of sequence divergence (uncorrected *P*) among *L. coronata* haplotypes ranged from 0 to 5.53%. Within major lineages, mean sequence divergence values were less than 1%, ranging from 0.43 to 0.86%. Among lineages, mean sequence divergence values ranged from 1.45% (Napo/Marañon populations versus north Amazon populations) to 4.25% (*cis*-Andean populations versus *trans*-Andean populations) (Table 1).

There was no significant difference in phylogenetic signal among codon positions across all protein-coding partitions ($P = 0.18$), suggesting that the third codon position has not become saturated. Furthermore, the maximum percent sequence divergence value is 5.53%, well below the level (~10%) at which saturation at the third codon position generally becomes a problem. Partition-homogeneity tests failed to reject the null hypothesis of homogeneous phylogenetic signal in all pair-wise comparisons of protein-coding partitions (ND2 versus ND3, $P = 0.29$; ND2 versus cytochrome *b*, $P = 0.39$; ND3 versus cytochrome *b*, $P = 0.80$).

Table 1
Mean and range of percentage of sequence divergence within and among *L. coronata* lineages

Comparison	Uncorrected pair-wise % (range)	Kimura 2-parameter/Γ% (range)
Within lineages		
Napo/Marañon	0.59 (0.00–1.32)	0.64 (0.00–1.39)
North Amazon	0.43 (0.09–0.80)	0.40 (0.00–1.44)
Central Peru	0.86 (0.09–1.87)	0.90 (0.09–1.81)
South Peru/Bolivia	0.61 (0.09–1.41)	0.64 (0.09–1.48)
Venezuela	0.85 (0.00–1.78)	0.88 (0.00–1.93)
trans-Andean	0.76 (0.00–1.78)	0.80 (0.00–1.91)
Among lineages		
Napo/Marañon vs. North Amazon	1.45 (0.66–2.14)	1.48 (0.68–2.35)
Central Peru vs. South Peru/Bolivia	1.84 (1.50–2.53)	1.93 (1.19–2.72)
North Amazonia vs. South Amazonia	2.88 (2.44–3.47)	3.15 (1.87–4.16)
Amazonia vs. Venezuela	4.01 (3.03–4.87)	4.83 (3.86–6.31)
cis-Andean vs. *trans*-Andean	4.25 (3.04–5.53)	5.43 (3.61–7.32)

Lineages correspond to Fig. 2 and text.

3.2. Maximum parsimony analysis

Parsimony analysis resulted in 38 most parsimonious trees (length = 378, CI = 0.7037, RI = 0.8848; one of these, with bootstrap values derived from the 50% majority rule consensus, is shown in the supplemental material). The monophyly of *L. coronata* lineages was well supported with 91% bootstrap support and the analysis also recovered six major haplotype clades (*trans*-Andean, Venezuela, North Amazon, Napo-Marañon, Central Peru, and South Peru/Bolivia) all of which were well supported with 89–100% bootstrap support. The *trans*-Andean (west of Andes including Central America) clade was placed basally with 91% bootstrap support. Among the *cis*-Andean (east of the Andes) clades, the Venezuela clade was basal with 75% bootstrap support. A North Amazonia clade consisting of populations north of the Amazon and Marañon rivers was sister to a South Amazonia clade consisting of populations south of these rivers with 95% bootstrap support. Both of these clades were well supported with 96 and 100% bootstrap support, respectively. The North Amazonia clade was divided into two sister clades, one bounded by the Napo and Marañon rivers (the Napo/Marañon clade—90% bootstrap support) and the other consisting of Peruvian populations north of the Amazon River (the North Amazon clade—98% bootstrap support). The South Amazonia clade was also divided into two sister clades. One was a Central Peru clade consisting of populations from the south bank of the Amazon

River and the Peruvian departments of southern Loreto, Ucayali, and San Martín (89% bootstrap support). The other was a southern Peru/Bolivia clade consisting of populations from southern Peru, southwestern Brazil, and northern Bolivia (100% bootstrap support). Resolution and bootstrap values decrease dramatically towards the tips of major lineages, most likely due to a lack of informative variation.

3.3. Maximum likelihood analysis

Maximum likelihood analysis resulted in a most likely tree ($-\ln L = 3654.61$) (Fig. 2) that recovered the same six haplotype clades recovered in the parsimony analysis. Topologies between the two methods were identical at higher levels (among the major haplotype clades), and each of the clades as well as the overall topology was well supported (61–100% bootstrap support) in the ML analysis. Minor topological differences between the ML and MP trees existed at the higher, poorly supported nodes (within Amazonian haplotype clades).

3.4. Bayesian inference of phylogeny

Bayesian analysis also recovered the six major lineages and topology recovered by MP and ML analyses

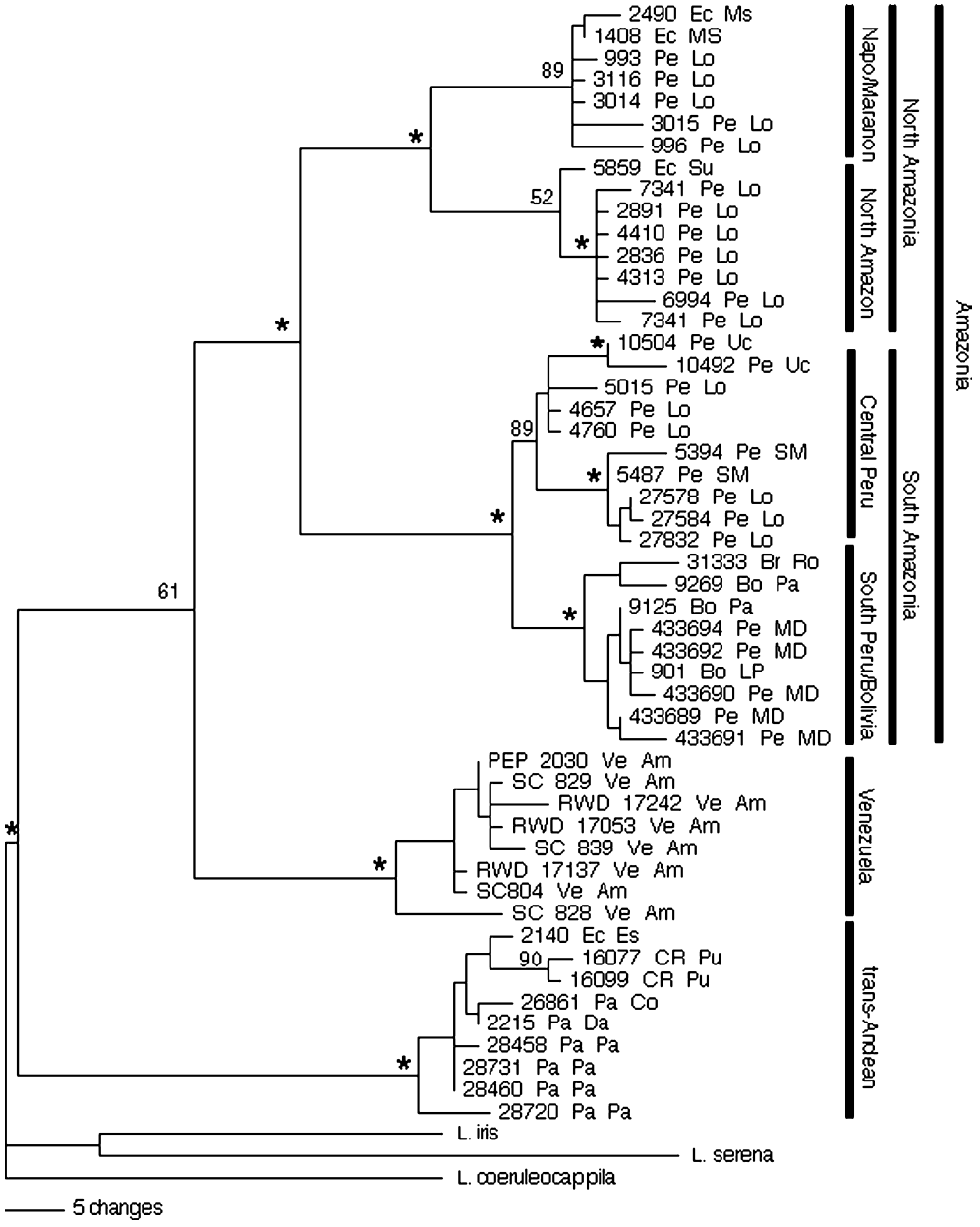

Fig. 2. Phylogenetic relationships among *L. coronata* haplotypes reveal a high degree of phylogeographic structure. The illustrated tree is a maximum likelihood tree based on an HKY + G model of evolution. Numbers above nodes are bootstrap values based on 100 non-parametric replicates. Nodes with bootstrap values $\geqslant 95\%$ are indicated with an asterisk. Clade distributions are illustrated in Fig. 1.

(supplementary information). Again, lineages and the relationships among them were well supported with posterior probabilities ranging from 72 to 100%. In fact, five of the six major lineages were supported with 100% posterior probability. Topological differences among MP, ML, and Bayesian analyses existed at poorly supported, lower level (within haplotype clade) nodes. These minor differences were most likely due to a lack of informative variation near the tips of the trees. The high degree of topological congruence and support for nodes estimated by the three methods suggests that the phylogeny of *L. coronata* haplotypes is robust.

3.5. Estimates of divergence times

Application of a substitution rate of 0.008 per site per lineage per million years (Fleischer et al., 1998) resulted in estimated divergence times among *L. coronata* lineages ranging from 0.49 (±0.21) to 2.3 (±1.0) million years before present (mybp). The earliest divergence occurred between the *cis*- and *trans*-Andean lineages and the latest divergence occurred between the Napo/Marañon and North Amazon lineages. Estimated divergence times among all haplotype clades are presented in Table 2.

3.6. Nested clade phylogeographical analysis

The nesting design for the three- to seven-step clades used in NCPA is presented in Fig. 3 and the haplotypes comprising lower nesting clades (1-, 2-, and 3-step clades) are given in Table 3. Three unconnected haplotype networks were recovered, corresponding to the *trans* -Andean, Venezuela, and Amazonia clades recovered in the phylogenetic analyses (Figs. 2 and 3). Within the three networks there are nine ambiguous connections, eight in clade 6-1AM (Amazonia clade) and one in clade 4-1TR (*trans*-Andean clade). All of these ambiguities involve connections to missing haplotypes and occur at the lowest (1 and 2 step) nesting levels.

Table 4 presents the results of the NCPA for *L. coronata*. The null hypothesis of no phylogeographic association between haplotypes and sampling location was rejected for seven clades. Included within these seven clades are the six major haplotype clades recovered in the phylogenetic analysis, suggesting a high degree of phylogeographic structure. The null hypothesis could not be rejected at nesting levels below the three-step level, which is indicative of either panmixia or inadequate geographic and/or genetic sampling at these nesting levels. There was significant structure within the

Table 2
Combined results of traditional phylogeographic analysis, NCPA, historical demographic analyses, and estimated divergence times reveal a complex evolutionary history for *L. coronata*

Node	Analysis	Result
trans- and *cis*-Andean	Phylogeography	Clades bordered by the Andes
	NCPA	Inadequate geographic sampling
	Demographic history[a]	—
	Estimated divergence time	2.3 ± 1.0 mybp
Venezuela and Amazonia	Phylogeography	Clades not separated by contemporary barrier
	NCPA	Inadequate geographic sampling
	Demographic history[a]	—
	Estimated divergence time	2.0 ± 0.9 mybp
North and South Amazonia	Phylogeography	Clades separated by Amazon and Marañon rivers
	NCPA	Allopatric fragmentation
	Demographic History	North Amazonia—equilibrium[b]
		South Amazonia—expansion[c]
	Estimated divergence time	1.4 ± 0.64 mybp
Central Peru and South Peru/Bolivia	Phylogeography	Clades not separated by contemporary barrier
	NCPA	Contiguous range expansion
	Demographic history	Central Peru—expansion[c]
		South Peru/Bolivia—expansion[c]
	Estimated divergence time	0.65 ± 0.34 mybp
Napo/Marañon and North Amazon	Phylogeography	Clades separated by Napo river
	NCPA	Allopatric fragmentation
	Demographic history	Napo/Marañon—equilibrium[b]
		North Amazon—equilibrium[b]
	Estimated divergence time	0.49 ± 0.21 mybp

Results are given within the context of nodes representing divergence among major *L. coronata* haplotype lineages.

[a] Demographic history was not inferred for these nodes (see Section 2).

[b] Fu's F_s and R_2 values were non-significant for both clades (Napo/Marañon and North Amazon) comprising the North Amazonia clade. But the mismatch distribution of the North Amazon clade was characteristic of demographic expansion.

[c] Fu's F_s was significantly negative and mismatch distributions were characteristic of a rapid demographic expansion for both clades (Central Peru and South Peru/Bolivia) comprising the South Amazonia clade.

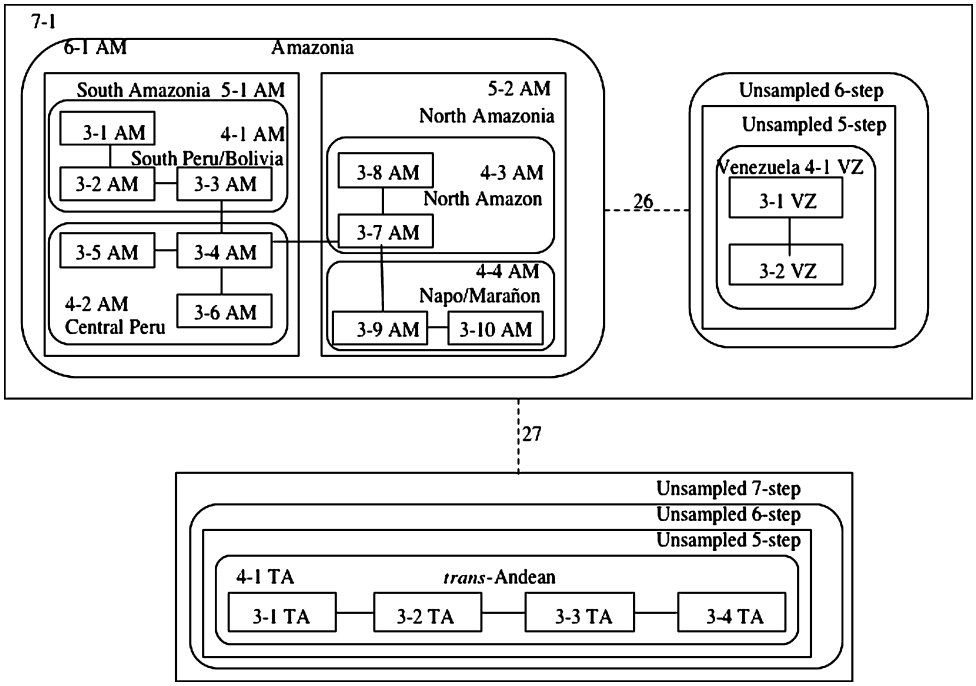

Fig. 3. Phylogeographic structure is corroborated by the results of NCPA. Illustrated is the nesting design for the three- to seven-step clades; note that each of the six haplotype clades recovered by phylogenetic analysis is supported as a higher level clade in NCPA. Solid lines connecting haplotype clades represent single mutational steps. Numbers beside dashed lines represent the minimum number of steps necessary to join the unconnected networks. In all clade designations, the first number refers to the nesting level and the second distinguishes it from other clades at the same nesting level. Haplotypes comprising the 1-, 2-, and 3-step clades are given in Table 2.

trans-Andean and Amazonia clades but not within the Venezuela clade (Fig. 3 and Table 4). The inferred evolutionary processes responsible for the observed phylogeographic structure are given in Table 4. Single processes were inferred for four of the seven clades with significant phylogeographic structure; however, the inferred cause of divergence differed among these clades. Allopatric fragmentation was the inferred cause of divergence between clades 5-1AM and 5-2AM nested within clade 6-1AM as well as clades 4-3AM and 4-4AM nested within clade 5-2AM (Table 4). Contiguous range expansion was inferred for clade 5-1AM, whereas restricted gene flow with isolation by distance was the inferred cause of divergence between clades 3-1TA, 3-2TA, 3-3TA, and 3-4TA nested within clade 4-1TA. Inadequate geographic sampling prevented inference of the cause of structure for the remaining three clades, likely resulting from the lack of tissue samples from Colombia.

3.7. Historical demographic analysis

Significance of Fu's F_s varied among clades. Values were significantly negative ($\alpha = 0.05$) for the Venezuela, Central Peru, and South Peru/Bolivia clades, suggesting rapid demographic expansion in these clades. Values were non-significant for the *trans*-Andean, Napo/Marañon, and North Amazon clades, suggesting relatively stable demographic histories for these lineages (Table 5). Values for the R_2 statistic also varied among clades, but only the value for the South Peru/Bolivia clade was significant (Table 5). Mismatch distributions also differed considerably among clades (Fig. 4). The distributions for the North Amazon, Central Peru, and South Peru/Bolivia lineages were more characteristic of the smooth Poisson distribution expected for populations that have experienced a demographic expansion. Moreover, the distributions for these clades had low raggedness (Harpending, 1994) values, again indicative of demographic expansion. Conversely, the distributions of the *trans*-Andean, Venezuela, and Napo/Marañon lineages were much more ragged, as indicated by higher raggedness indices, suggesting relatively stable demographic histories for these populations. A model of rapid demographic expansion could not be rejected for any of the clades (Table 5). Given the variation in Fu's F_s, R_2 (Table 5), and the shape of the mismatch distributions (Fig. 4), however, this is most likely due to a lack of statistical power for those clades with obviously ragged distributions.

3.8. Nucleotide diversity

Levels of nucleotide diversity (π) differed considerably among sampling sites, with site 15 being the most diverse ($\pi = 0.0066 \pm 0.005$) and site 1 being the least ($\pi = 0$) (Fig. 5). Centers of nucleotide diversity are

Table 3
Haplotypes comprising 1-, 2-, and 3-step clades of NCPA

Haplotype	1-step clade	2-step clade	3-step clade
Amazonia			
31333 Br Ro	1-1AM	2-1AM	3-1AM
9269 Bo Pa	1-2AM	2-2AM	—
433691 Pe MD	1-3AM	2-3AM	3-2AM
433693 Pe MD	1-4AM	2-4AM	—
9125 Bo Pa	—	—	—
901 Bo LP	1-5AM	2–5AM	—
433694 Pe MD	—	—	—
433692 Pe MD	—	—	—
433690 Pe MD	1-6AM	—	—
9177 Bo Pa	1-7AM	2-6AM	3-3AM
4657 Pe Lo	1-8AM	2-7AM	3-4AM
4760 Pe Lo	1-9AM	—	—
5015 Pe Lo	1-10AM	2-8AM	—
10492 Pe Uc	1-11AM	2-9AM	3-5AM
10504 Pe Uc	1-12AM	2-10AM	—
11087 Pe Uc	—	—	—
11070 Pe Uc	1-13AM	—	—
5487 Pe SM	1-14AM	2-11AM	3-6AM
5490 Pe SM	—	—	—
27832 Pe Lo	1-15AM	2-12AM	—
27578 Pe Lo	1-16AM	—	—
27584 Pe Lo	—	—	—
5394 Pe Lo	1-17AM	2-13AM	—
6994 Pe Lo	1-18AM	2-14AM	3.7AM
4410 Pe Lo	1-19AM	2-15AM	—
2891 Pe Lo	—	—	—
2742 Pe Lo	—	—	—
7341 Pe Lo	1-20AM	—	—
4313 Pe Lo	1-21AM	2-16AM	3-8AM
7347 Pe Lo	1-22AM	—	—
2836 Pe Lo	1-23AM	—	—
5859 Pe Lo	1-24AM	2-17AM	—
3116 Pe Lo	1-25AM	2-20AM	3-9AM
3014 Pe Lo	1-26AM	—	—
996 Pe Lo	1-27AM	2-21AM	—
3015 Pe Lo	1-28AM	2-18AM	3-10AM
1408 Ec MS	1-29AM	2-19AM	—
2490 Ec MS	1-30AM	—	—
Venezuela			
RWD17137 Ve Am	1-1VZ	2-1VZ	3-1VZ
SC804 Ve Am	—	—	—
PEP2030 Ve Am	1-2VZ	—	—
SC839 Ve Am	1-3VZ	2-2VZ	—
SC772 Ve Am	1-4VZ	—	—
SC829 Ve Am	—	—	—
RWD17053 Ve Am		—	—
RWD17242 Ve Am	1-5VZ	—	—
SC828 Ve Am	1-6VZ	2-3VZ	3-2VZ
SC749 Ve Am	—	—	—
GFB2190 Ve Am	—	—	—
trans-*Andean*			
16099 CR Pu	1-1TA	2-1TA	3-1TA
16077 CR Pu	1-2TA	—	—
2140 Ec Es	1-3TA	2-2TA	3-2TA
28720 Pa Pa	1-4TA	2-3TA	—
2215 Pa Da	1-5TA	2-4TA	3-3TA
26860 Pa Co	—	—	—
26861 Pa Co	1-6TA	—	—
28731 Pa Pa	1-7TA	2-5TA	3-4TA
28458 Pa Pa	1-8TA	—	—

Relationships among higher level (3- to 7-step) clades are illustrated in Fig. 3. Haplotype codes correspond to Appendix A. Dashes indicate membership in the above clade.

associated with each of the Venezuela, Napo/Marañon, and South Peru/Bolivia clades. Within the larger North Amazonia clade there is an apparent eastward decline in diversity from site 15. The highest degree of diversity in the larger South Amazonia clade is associated with one of the southernmost sites (site 27).

4. Discussion

Phylogenetic analyses recovered six well-supported haplotype clades within *L. coronata*, and their distributions reveal a high degree of phylogeographic structure within the species. The following sections will discuss the evolutionary implications and inferences drawn from the combined results of NCPA, historical demographic, and classic phylogeographic analyses (summarized in Table 2) within the context of the major haplotype lineages and nodes representing divergence events among lineages.

4.1. Congruence between phylogeographic structure and subspecific taxonomy

Lepidothrix coronata consists of eight subspecies (Traylor, 1979), which were described on the basis of differences in adult male plumage. Phylogenetic analyses revealed six reciprocally monophyletic haplotype clades, allowing for the assessment of congruence between genetic breaks and subspecific taxonomy, and more generally, assessment of congruence between patterns of genetic and male plumage variation. Seven of the eight subspecies were sampled, and of these, only one, *L. c. carbonata* of southern Venezuela, was monophyletic in terms of its haplotype relationships. Thus, all but one of the described subspecies are not supported as natural groups by these molecular data, suggesting that current taxonomy may not accurately reflect phylogeny. This conclusion, however, is best treated as tentative. Sex-biased introgression or dispersal can yield misleading mtDNA patterns (Paetkau et al., 1998) and we cannot eliminate the possibility that variation at other loci may be more congruent with subspecific taxonomy.

One of the most striking results is the lack of congruence between plumage similarity and phylogenetic affinity, which is most vividly illustrated by the Central Peru clade. This clade includes males that are entirely black (typical of *L. c. coronata*) from the south bank of the Amazon (site 22) and males that are primarily green (typical of the green subspecies *L. c. exquisita*) from central Peru (site 23), as well as males representing various intergrades between the green and black plumage groups (sites 24 and 25). Despite this variation in plumage, these individuals form a well-supported monophyletic haplotype clade, to the exclusion of other "pure" black and green haplotype clades. Conversely, birds from the north bank of the Amazon look identical to those from the

Table 4
NCPA results for *L. coronata*

Clade	χ^2 statistic	Probability	Inference chain	Inferred process
trans-*Andean*				
4-1TA	31.00	0.0212	1-2-3-4-NO	Restricted gene flow with isolation by distance
Venezuela				
None				
Amazonia				
Clade 4-2AM	25.00	0.0004	1-19-20-NO	Inadequate geographic sampling
Clade 5-1AM	**23.00**	**0.0000**	**1-19-20-2-11-YES**	**Contiguous range expansion**
Clade 5-2AM	**17.00**	**0.0002**	**1-19-NO**	**Allopatric fragmentation**
Clade 6-1AM	**39.00**	**0.0000**	**1-19-NO**	**Allopatric fragmentation**
Clade 7-1AM	**56.00**	**0.0000**	**1-19-20-NO**	**Inadequate geographic sampling**
Total cladogram				
Total	**62.00**	**0.0000**	**1-19-20-NO**	**Inadequate geographic sampling**

The inferred causes of divergence among the six major haplotype clades are in bold.

Table 5
Results of historical demographic analyses

Clade	*n*	Raggedness	*P* (Raggedness)	R_2	*P* (R_2)	Fu's F_s	*P* (Fu's F_s)
trans-Andean	12	0.0803	0.451	0.1495	0.441	0.05	0.50
Venezuela	11	0.0344	0.867	0.1271	0.227	−4.527	0.011
Napo/Marañon	7	0.3200	0.258	0.1447	0.094	−1.311	0.148
North Amazon	10	0.0610	0.834	0.1153	0.056	−1.164	0.115
Central Peru	13	0.0128	0.995	0.1076	0.085	−6.223	0.004
South Peru/Bolivia	11	0.0845	0.890	0.0845	0.005	−5.844	0.001

Raggedness values are measures of the smoothness of the mismatch distributions. Smooth Poisson mismatch distributions are characteristic of rapid demographic expansion. *P* (Raggedness) are the probabilities of observing a distribution with higher raggedness based on 1000 coalescent simulations. Low R_2 values and negative Fu's F_s values are also indicative of demographic expansion. *P* (R_2) and *P* (Fu's F_s) is the probability of an R_2 and F_s value being less than the observed based on 1000 coalescent simulations.

south bank, yet a relatively large genetic break (3.2%, Table 1) exists between them. Similarly, birds from southern Venezuela are morphologically most similar to those from northern Peru, although they do belong to different subspecific taxa, *L. c. carbonata* and *L. c. coronata*, respectively. In the type description of *carbonata*, Todd (1925) suggests that it can be distinguished from *coronata* by its "deeper, blacker coloration." This distinction, however, is not obvious in comparisons of series of specimens and despite the close similarity in plumage, these populations are among the most highly divergent (~4%, Table 1) of all clades within the species (Table 1). This apparent discordance between plumage color and phylogenetic affinity may be the result of a number of factors including introgression, incomplete lineage sorting, and geographically variable selective constraints on male plumage color. Distinguishing among these alternatives will require data from nuclear loci and further understanding of the role of plumage coloration in Blue-crowned Manakin behavior.

4.2. Congruence between ecogeographic barriers and genetic breaks within L. coronata

The distribution of *L. coronata* encompasses several potential geographic barriers, including the Andes and major rivers within the Amazon basin (Fig. 1). Of the six haplotype lineages, the distributions of three are delimited by obvious contemporary barriers. At the basal node, the distributions of the *cis*- and *trans*-Andean clades are delimited by the Mérida Andes, Sierra de Perija, and Eastern Cordillera of the northern Andes. This biogeographic pattern is not surprising and is consistent with patterns recovered many in other phylogenetic studies of Neotropical birds (Bates et al., 1998; Brumfield and Capparella, 1996; Cracraft and Prum, 1988; Marks et al., 2002; Prum, 1988). The basal position of the *trans*-Andean clade and estimated divergence times (Table 2), however, suggest that the Amazonian radiation occurred after the final uplift of the northern Andes.

Rivers can be important barriers to gene flow for birds that are restricted to the understory of unflooded (*terra firme*) forest (Aleixo, 2004; Capparella, 1988). At least three rivers appear to be important barriers influencing the genetic structure of *L. coronata*. The Amazon River separates the distributions of North Amazonia and South Amazonia clades; and the Napo and Marañon rivers, major tributaries of the Amazon, delimit the distribution of the Napo/Marañon clade (Fig. 1). Given the deep phylogenetic structure and estimated divergence times associated with these nodes, it is likely that

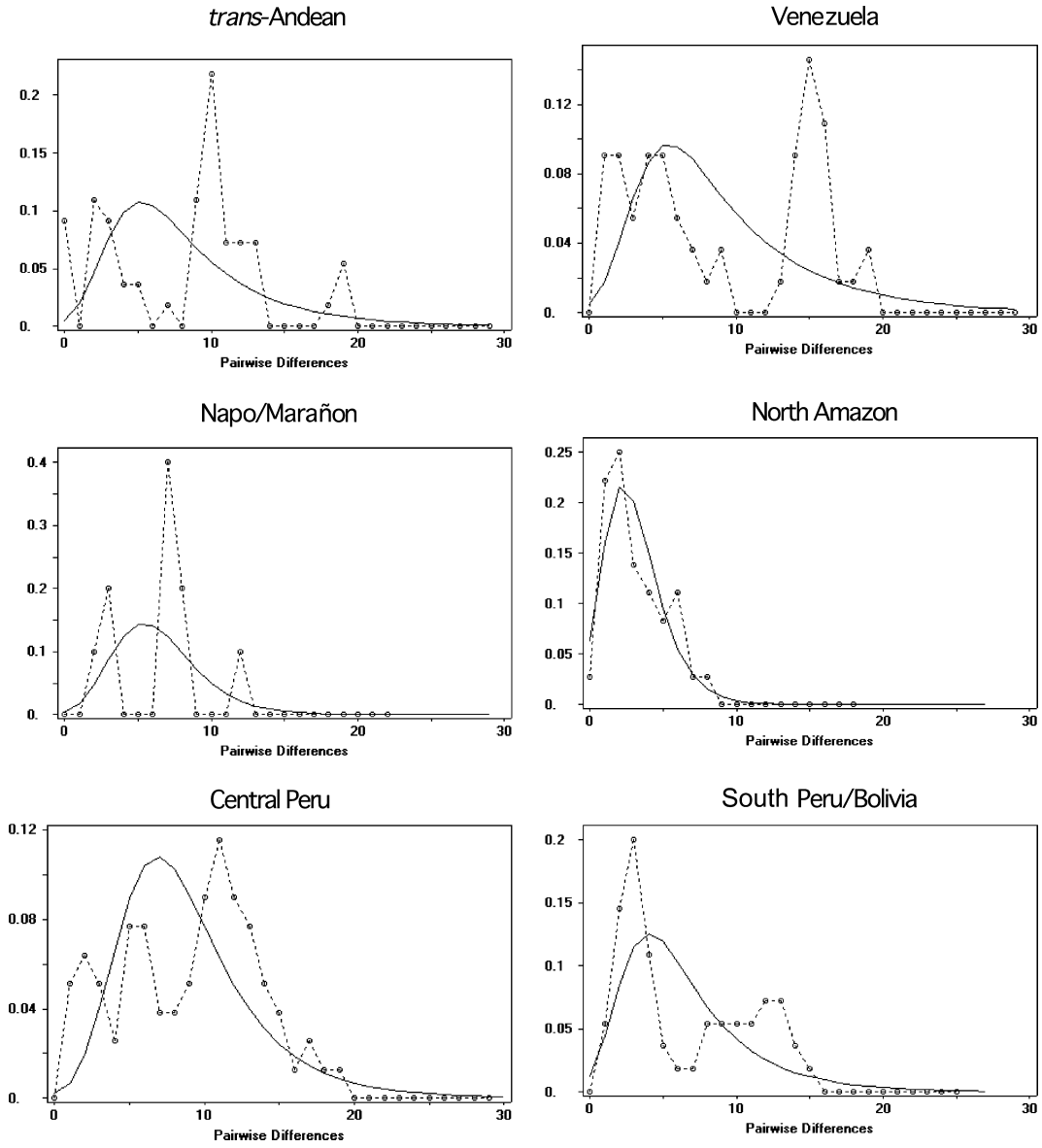

Fig. 4. Mismatch distributions reveal variation in the demographic histories of *L. coronata* haplotype clades. Illustrated are the frequency distributions of pair-wise nucleotide difference between *L. coronata* individuals within haplotype clades. Dashed lines represent observed data. Solid lines represent expected values under a model of demographic expansion fitted to the observed data.

these rivers have been barriers for much of the evolutionary history of *L. coronata*. However, the importance of another major tributary of the Amazon, the Ucayali River, is unclear. The distribution of the Central Peru clade crosses the Ucayali (Fig. 1), and there are differences in haplotype frequencies on opposite banks. However, NCPA did not detect significant phylogeographic structure at this level. The lack of significant phylogeographic structure in conjunction with the poor phylogenetic resolution within the Central Peru clade makes us reluctant to split it into two clades separated by the Ucayali despite the differences in haplotype frequency occurring on its banks. Further work is needed to determine the importance of the Ucayali as a barrier for these birds. In general, determining which rivers in the Amazon basin are barriers to a wide range of taxa will be of great interest to evolutionary and conservation biologists alike.

When contemporary ecogeographic barriers delimit the distributions of sister taxa, it is tempting to attribute divergence to the formation of the barrier. It is often unclear, however, whether the barrier is the cause of divergence (primary barrier), or whether it merely limits current distributions (secondary barrier). Formation of both the Andes and the Amazonian river system have been hypothesized as important vicariant events in the evolution of Neotropical birds (Capparella, 1988, 1991; Chapman, 1917; Sick, 1967). Thus an important

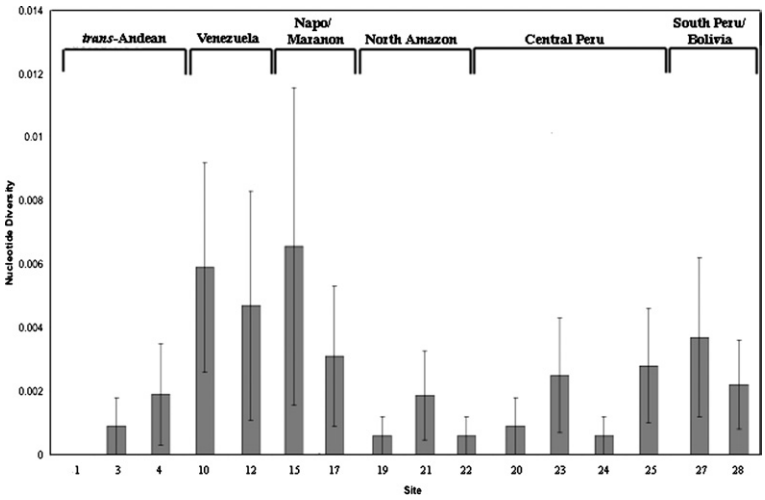

Fig. 5. Levels of nucleotide diversity (π) vary geographically. Sites are arranged north to south by clades, and sites where only one individual was sampled are excluded. Site numbers correspond to Fig. 1 and Appendix A.

evolutionary question is whether the barriers identified for *L. coronata* are primary or secondary in nature. This question is difficult to address using classic phylogeographic approaches alone, because the phylogeographic prediction is the same; that is, sister taxa should occur on opposite sides of the barrier (Voelker, 1999). However, NCPA and historical demographic analyses provide insights into the processes that have shaped phylogeographic structure. The combination of these process-level inferences with classical phylogeography allows for a more robust analysis of the role of ecogeographic barriers.

Inherent in the hypothesis that a barrier is secondary rather than primary is the hypothesis that the taxa involved must have experienced a range expansion to come in contact with the barrier. Thus, clades separated by a secondary barrier should exhibit evidence of a rapid range expansion, whereas those separated by a primary barrier should not, because the initial cause of divergence continues to limit clade distributions. This is assuming, of course, that there have been no major habitat alterations on either side of a primary barrier that could cause population bottlenecks. Given these interrelated hypotheses, four predictions can be made for secondary barriers:

(1) *Common haplotypes and their evolutionary descendants should have large geographic distributions (Hewitt, 1996, 2000; Templeton et al., 1995).* With any founder event, only a subset of the standing genetic variation within the ancestral population is represented in the smaller colonizing population. Common haplotypes are most likely to be involved in a range expansion and thus may be expected to have large geographic distributions relative to common haplotypes in stable populations.

(2) *An abundance of closely related, derived haplotypes should occur near the barrier (Templeton et al., 1995).* The relative abundances of ancestral and derived haplotypes can provide insight into the relative ages of populations. Specifically, as noted above in prediction 1, common haplotypes are most likely to be involved in a range expansion. With reduced gene flow between the ancestral and colonized population, derived haplotypes arising within the colonized population will remain geographically confined and should be closely related to one another (i.e., separated by few mutational steps). Because only a subset of the ancestral variation is present in the colonizing population, such populations may be recognized by a higher proportion of closely related, derived haplotypes that are the descendants of colonizing ancestral haplotypes (Hewitt, 1996, 2000). These colonized populations should occur near a secondary barrier, concordant with a range expansion to the barrier.

(3) *Genetic patterns characteristic of demographic expansion (associated with range expansion) should be recovered (Lessa et al., 2003; Zink et al., 2000).* Because range expansions are accompanied by demographic expansions, populations separated by secondary barriers should exhibit the genetic signatures of rapid demographic expansion.

(4) *Levels of genetic diversity should decrease as they approach the barrier (Hewitt, 1996, 2000).* Lowered genetic diversity in colonizing populations relative to ancestral populations is a well-established pattern (Hewitt, 2000). This is because only a subset of the standing genetic diversity in the ancestral population will be represented in the colonizing population. Thus, levels of genetic diversity should decrease as they approach a secondary barrier in concordance with the direction of colonization.

The first two predictions are incorporated into inferences of range expansion in NCPA (Templeton et al., 1995; Templeton, 2004). The third prediction may be tested through the historical demographic analyses employed here, and the fourth, by examining patterns of geographic variation in nucleotide diversity.

Divergence patterns among *L. coronata* haplotype lineages reveal three primary ecogeographic barriers. The Napo River in northeastern Peru and Ecuador separates two sister clades, the Napo/Marañon clade and the North Amazon clade (Fig. 1). In the NCPA, these clades correspond to clades 4-3AM and 4-4AM nested within clade 5-2AM (Fig. 3). Allopatric fragmentation is the inferred process at this node (Table 4), because the distributions of these clades are entirely non-overlapping and relatively large mutational differences separate them (Templeton, 2004). This result is consistent with the Napo River being a primary barrier, and this inference is corroborated by the results and patterns of the historical demographic analyses. Both Fu's F_s and R_2 values were non-significant for both clades (Table 2) and the ragged mismatch distribution of the Napo/Marañon clade (Fig. 4) is characteristic of a stable demographic history as predicted for primary barriers. However, the Napo/Marañon clade is characterized by relatively high levels of nucleotide diversity, whereas nucleotide diversity within populations comprising the North Amazon clade is among the lowest of all populations within the species (Fig. 5). This pattern can be considered to be consistent with expansion from a smaller ancestral population and possible dispersal across the Napo (Hewitt, 1996, 2000), which is corroborated by the smooth mismatch distribution for the North Amazon clade. However, given the natural history of the bird it seems unlikely that it would be able to disperse across such a major barrier (Ridgley and Tudor, 1994; Snow, 2004). A more likely explanation is that the North Amazon clade experienced a population bottleneck after the two populations were fragmented by the formation of the Napo River. On the whole, the results at this node support the Napo River as a primary barrier leading to the divergence between the Napo/Marañon and North Amazon clades.

The Amazon River also separates a pair of sister clades, the North Amazonia clade and South Amazonia clade. These groups correspond to clades 5-1AM and 5-2AM nested within clade 6-1AM in the NCPA. Haplotypes sampled from the south bank of the Amazon occupy interior positions in the nested cladogram relative to haplotypes sampled from south Peru and Bolivia, suggesting that these haplotypes are ancestral within the South Amazonia clade (Templeton et al., 1995). These ancestral haplotypes were sampled on the south bank of the Amazon River, whereas only derived haplotypes were sampled in the southern portion of the range. This pattern is directly opposite of that predicted for a northward expansion to the south bank of the Amazon as would be expected if it were a secondary barrier and the southern populations were ancestral. The non-overlapping ranges and large mutational distances between the two clades, led to the inference of allopatric fragmentation in NCPA, a result that is consistent with the Amazon being a primary barrier; historical demographic analyses corroborate these phylogeographic patterns. Values of Fu's F_s and R_2 were non-significant for both clades north of the Amazon River (Table 5, Fig. 4), indicating that these clades have experienced a relatively stable recent demographic history. Both clades south of the Amazon, however, had significantly negative values for Fu's F_s suggesting that these populations have experienced a recent demographic expansion. The combined results suggest that the Amazon river acted as a primary barrier leading to the divergence of the North and South Amazonia clades and that this initial divergence was followed by a southward expansion in the South Amazonia clade, a scenario that is supported by the NCPA inference of contiguous range expansion at a lower nesting level within the South Amazonia clades (see next section).

Finally, the Andes separate the sister *cis*- and *trans*-Andean clades. NCPA was uninformative at this level due to inadequate geographic sampling, and historical demographic analyses were inappropriate because they would have required combining the divergent Amazonian lineages into a single *cis*-Andean clade (see Section 2). Thus we cannot use these analyses to compare sister clades on opposite sides of the Andes. However, the demographic analyses indicate that the *trans*-Andean clade has experienced a relatively stable demographic history as predicted for primary barriers (Table 5, Fig. 4). Moreover, the Andes have been inferred as a primary barrier for several avian taxa (Bates et al., 1998, 1999; Brumfield and Capparella, 1996; Cracraft and Prum, 1988; Marks et al., 2002; Prum, 1988) and given the relatively low vagility and lowland forest habitat restrictions of *L. coronata*, it is very likely that the Andes represent a primary barrier for the Blue-crowned Manakin as well.

4.3. Genetic breaks in the absence of ecogeographic barriers

In addition to the phylogeographic structure associated with contemporary barriers, two major genetic breaks occur in the absence of any obvious ecogeographic barrier. The break between the Central Peru and South Peru/Bolivia clades occurs in continuous forest in southern Loreto and northern Madre de Dios departments of Peru (Fig. 1). This pattern is consistent with phylogeographic patterns recovered for another widespread bird, the Wedge-billed Woodcreeper (*Glyphorynchus spirurus*) (Marks et al., 2002). Likewise, the split between the Venezuela and Amazonia clades also occurs in continuous forest. However, in this case we are unable to precisely locate

clade boundaries due to the lack of available samples from Colombia and northwestern Brazil.

Although we acknowledge that the structure in these areas could be the result of more subtle contemporary ecological barriers, we argue that this is unlikely. Both of these genetic breaks are estimated to be relatively old, at least 310,000 years for the Central Peru and South Peru/Bolivia split and at least 1.1 mybp for the Venezuela and Amazonia split. Given the climatic fluctuation of the Pleistocene (Bush, 1994; Colinvaux et al., 1996; Colinvaux and De Oliveira, 2000) it is unlikely that any contemporary ecological barriers would have remained unaltered over these time scales. The more likely explanation is that these genetic breaks are relicts of historical vicariant events. Several historical hypotheses evoke vicariant mechanisms including the refugia hypothesis (Haffer, 1969, 1974, 1997), the disturbance-vicariance hypothesis (Bush, 1994; Colinvaux, 1993, 1998; Colinvaux et al., 1996) and the marine transgression hypothesis (Nores, 1999; Webb, 1995). Each of these hypotheses may predict phylogeographic structure in the absence of a contemporary barrier and the genetic footprint of rapid range and demographic expansion.

Based on the results of NCPA, contiguous range expansion is the inferred cause of structure at the Central Peru and South Peru/Bolivia node. Because haplotypes associated with the Central Peru clade occupy ancestral (interior) positions in the nested cladogram relative to those associated with the South Peru/Bolivia clade, it can be reasonably inferred that the expansion was southward from an ancestral population located somewhere within the current distribution of the Central Peru clade (Fig. 1). This interpretation is corroborated by the historical demographic analyses. Values for Fu's F_s are significantly negative, indicative of a rapid demographic expansion. Moreover, the mismatch distributions for both clades are characteristic of demographic expansion (Fig. 4). These results support a scenario of expansion from a refugial population at this node.

Inferring the cause of structure at the Venezuela and Amazonia node is more difficult. Unfortunately, NCPA was uninformative at this level due to inadequate geographic sampling and comparisons of demographic histories between the sister Venezuela and Amazonia clades would have required combining the divergent Amazonian lineages into a single clade (see Section 2). Insight into this divergence, however, can be gained from timing of the *cis*-Andean splits inferred from the branching pattern of the phylogeny and estimated divergence times. The initial divergence in the *cis*-Andean radiation is the split between the Venezuela and the Amazonian lineages (Fig. 2). Divergence of the Amazonian lineages is estimated to have begun 600,000 years later (North and South Amazonia split—Table 2), suggesting that the event that led to the divergence of the Venezuela and Amazonian clades did not affect western Amazonia to a great extent. Congruent patterns in other phylogenetically widespread taxa (butterflies—Hall and Harvey, 2002; mammals—Hoffman and Baker, 2003; birds—Bates et al., 1998; Marks et al., 2002), including several strong-flying birds (Cracraft and Prum, 1988), implicate a major vicariant event that affected a wide range of taxa, including those with relatively high dispersal capabilities.

The phylogeographic patterns at these nodes support a history of past fragmentation and subsequent range expansion. Several plausible historical mechanisms exist to explain these patterns, the relative merits of which remain controversial (Colinvaux and De Oliveira, 2000). These hypotheses, however, are indistinguishable with respect to our data and the analyses we employed. Each hypothesis evokes "refugia," differing only in the intervening barrier, making the genetic footprints of these hypotheses identical.

4.4. Implications for historical hypotheses of the origin of Neotropical bird diversity

Nearly all hypotheses of the origin of Neotropical biodiversity are based on patterns of geographic variation within morphologically distinct taxa. For birds specifically, these patterns are defined almost entirely on the basis of patterns of plumage variation within species or among closely related species. Our data add to a growing body of evidence demonstrating a degree of discordance between plumage patterns and genealogical history (reviewed in Zink, 2004). Because both natural and sexual selection heavily influence avian plumage, such discordance between plumage and genetic characters should be expected in many cases. It is prudent to treat this pattern of discordance as preliminary, as most data sets demonstrating discordance are based on a single locus, but these data nonetheless force the question as to whether these hypotheses are explaining the appropriate pattern.

Most discussions of the origin of Neotropical avian biodiversity generally approach the problem from an historical perspective and nearly all attribute diversity to a single vicariant mechanism (reviewed in Haffer, 1997). Whereas an historical perspective may be appropriate, the data presented here suggest that historical hypotheses evoking a single mechanism of diversification are likely to be overly simplistic. A general prediction of such single-process historical hypotheses is that patterns recovered at each node should be similar and indicative of one overarching process. Such congruence among nodes was not supported by these data (Table 2). Instead, patterns differ at all nodes suggesting a complex evolutionary history for the Blue-crowned Manakin. Taken together, these data suggest that several vicariant processes including Andean uplift, formation of riverine barriers, and vegetational shifts associated with climatic

fluctuations, as well as a non-vicariant process, range expansion, may have all played a role in shaping the genetic structure of *L. coronata*. We suggest that comparative studies of taxa employing similar methods be used to test for congruent phylogeographic patterns, allowing for the placement of spatial, temporal, and perhaps sequential limits on hypothesized vicariant events.

A final issue is that of the timing of avian diversification in the Neotropics. Most historical hypotheses are based on Quaternary timescales; moreover, geological arguments refuting or supporting these hypotheses are generally based on data from the late Quaternary (~10,000–40,000 bp) (e.g., Bush et al., 1990; Colinvaux et al., 1996, 2000; Colinvaux, 1987, 1993; Haffer, 1969, 1997; Hooghiemstra and van der Hammen, 1998; Liu and Colinvaux, 1985; but see Rasanen et al., 1995; Webb, 1995). The data presented here add to a growing body of evidence suggesting that genetic structure within Neotropical bird species is generally older than late Quaternary in origin (reviewed in Mortiz, 2000; Bates et al., 2003; Marks et al., 2002). Such is the case for *L. coronata*, with the divergence between the *cis*- and *trans*-Andean lineages estimated to have occurred ~2.3 mybp. Although we are aware of the difficulties of estimating population divergence times on the basis of single locus gene trees (Edwards and Beerli, 2000), we are confident that at least some of the genetic structure in *L. coronata* is older than late Pleistocene in origin. The existence of this relatively old genetic structure within several avian species pushes the origin of these species into the Pliocene, or possibly even the Miocene. Thus, while interesting in their own right, arguments surrounding late Quaternary climatic or geological events may have little relevance to Neotropical avian diversification at the species level. Instead, events of the mid to late Pliocene may provide more insight into the historical factors shaping Neotropical avian diversity.

Acknowledgments

We gratefully acknowledge the following institutions and people for donating tissue samples and providing information on specimens in their collections (listed in alphabetical order by institution): Leo Joseph and Nate Rice, Academy of Natural Science, Philadelphia; Paul Sweet, American Museum of Natural History; John Bates and Dave Willard, Field Museum of Natural History; Mark Robbins, Kansas University Museum of Natural History; Josie Babin, Donna Dittmann, and Fred Sheldon, Louisiana State University Museum of Natural Science. We are especially grateful to the numerous collectors who endured difficult field conditions to procure the tissue samples used in this project. It is due to the tremendous efforts of these people that this project was possible. We thank John Bates who provided important insights during numerous discussions of the project. R.T. Brumfield, M.D. Carling, B. Counterman, S.S. Loew, B.D. Marks, M.A.F. Noor, D. Ortiz-Barrientos, W.L. Perry, C.C. Witt, and two anonymous reviewers provided many useful comments on earlier versions of the manuscript, greatly improving it. This work was supported by funding from the American Museum of Natural History Frank M. Chapman Memorial Fund, the American Ornithologists' Union Josselyn Van Tyne Fund, the Beta Lambda Chapter of the Phi Sigma Society R.D. Weigel Research Award and the E.L. Mockford Fellowship of Beta Lamba Chapter of the Phi Sigma Society of Illinois State University to Z.A.C.

Appendix A

Specimen information

Locality	Sample size	Tissue source	Tissue number	Haplotype code	GenBank Accession Nos. (ND3, ND2, cytochrome *b*)
1. Costa Rica: Puntarenas; Rio Copey, 4 km E Jaco, 9.62°, −84.63°	3	LSUMNS	16077	16077 CR PU	AY882094, AY882161, AY882224
			16099	16099 CR PU	AY882118, AY882185, AY882248
			16103[a]	16077 CR PU	AY882119, AY882186, AY882249
2. Panama: Panama Province, E Panama Canal, S Rio Chagres, Parque National Soberiania, 9.33°, −79.92°	1	LSUMNS	28460	28460 PA PA	AY882121, AY882188, AY882251
3. Panama: Colón Province; 17 km by road NW Gamboa, Rio Agua Salud, 9.22°, −79.67°	2	LSUMNS	26860[a]	26861 PA CO	AY882134, AY882201, AY882264
			26861	26861 PA CO	AY882110, AY882177, AY882240
4. Panama: Panama Province; Old Gamboa Road, 5 km NW Paraiso, 9.05°, −79.65°	2	LSUMNS	28720	28720 PA PA	AY882088, AY882155, AY882218
			28731	28731 PA PA	AY882113, AY882180, AY882243
5. Panama: Panama Province; Canal Area, Pacific side, 8.75°, −79.62°	1	LSUMNS	28458	28458 PA PA	AY882108, AY882175, AY882238
6. Costa Rica: Puntareans, Marenco Biological Station, 8.66°, −83.58°	1	LSUMNS	16121[a]	16077 CR PU	AY882095, AY882162, AY882225

(*continued on next page*)

Appendix A (*continued*)

Locality	Sample size	Tissue source	Tissue number	Haplotype code	GenBank Accession Nos. (ND3, ND2, cytochrome *b*)
7. Panama: Darién Province; Cana on E slope of Cerro Pirré, 7.75°, −70.67°	1	LSUMNS	2215	2215 PA PA	AY882117, AY882184, AY882247
8. Venezuela: Amazonas; Mavaca Base Camp, 2.37°, −65.12°	1	AMNH	GFB 2190[a]	SC828 VE AM	AY882098, AY882166, AY882229
9. Venezuela: Amazonas; Mrkapiwe, 2.16°, −66.5°	1	AMNH	PEP 2030	PEP2030 VE AM	AY882073, AY882140, AY882203
10. Venezuela: Amazonas; Rio Baria, 1.58°, −66.17°	6	AMNH	SC 749[a]	SC828 VE AM	AY882077, AY882144, AY882207
			SC 772[a]	SC828 VE AM	AY882092, AY882159, AY882222
			SC 804	SC804 VE AM	AY882075, AY882142, AY882205
			SC 828	SC828 VE AM	AY882076, AY882143, AY882206
			SC 829	SC829 VE AM	AY882079, AY882146, AY882209
			SC 839	SC839 VE AM	AY882120, AY882187, AY882250
11. Ecuador: Esmeraldas, 20 km NNW Alto Tambo, 0.95°, −77.5°	1	ANSP	2140[b]	2140 EC ES	AY882072, AY882139
12. Venezuela: Amazonas; Rio Mawarinumo, 0.92°, −66.17°	2	AMNH	RWD 17137	RWD17137 VE AM	AY882074, AY882141, AY882204
			RWD 17242	RWD17242 VE AM	AY882087, AY882154, AY882217
13. Ecuador: Sucumbios; ca. 20 km NE Lumbaqui, 0.25°, −77.25°	1	ANSP	5859[b]	5859 EC SU	AY882071, AY882138
14. Venzuela: Amazonas; San Carlos de Rio Negro, −2.08°, −66.48°	1	AMNH	RWD 17053	RWD17053 VE AM	AY882091, AY882158, AY882221
15. Peru: Loreto; San Jacinto, −2.3°, −75.85°	2	KUNHM	993	993 PE LO	AY882105, AY882172, AY882235
			996	996 PE LO	AY882132, AY882199, AY882262
16. Ecuador: Morona-Santiago; Santiago ca. 5 km SW Taisha, −2.37°, −77.5°	1	ANSP	2490[b]	2490 EC MS	AY882069, AY882136
17. Peru: Loreto; 1.5 km S Libertad, S bank of Rio Napo, 80 km N Iquitos, −3.03°, −72.75°	3	LSUMNS	3014	3014 PE LO	AY882114, AY882181, AY882244
			3015	3015 PE LO	AY882124, AY882191, AY882254
			3116	3116 PE LO	AY882085, AY882152, AY882215
18. Ecuador: Morona-Santiago; Santiago, −3.05°, −78.05°	1	ANSP	1408[b]	1408 EC MS	AY882070, AY882137
19. Peru: Loreto; 1 km N Rio Napo, 157 km by river NNE Iquitos, −3.27°, −73.08°	3	LSUMNS	2742[a]	2891 PE LO	AY882106, AY882173, AY882236
			2836	2836 PE LO	AY882112, AY882179, AY882242
			2891	2891 PE LO	AY882097, AY882164, AY882227
20. Peru: Loreto; S bank of Rio Amazonas, ca. 10 km SSW mouth of Rio Napo on E bank of Quebrada Vainilla, −3.42°, −72.58°	3	LSUMNS	4657	4657 PE LO	AY882131, AY882198, AY882261
			4760	4760 PE LO	AY882135, AY882202, AY882265
			5015	5015 PE LO	AY882109, AY882176, AY882239
21. Peru: Loreto; Rio Amazonas, 5 km ENE Oran, 85 km NE Iquitos, −3.58°, −72.75°	3	LSUMNS	6994	6994 PE LO	AY882126, AY882193, AY882256
			7341	7341 PE LO	AY882084, AY882151, AY882214
			7347	7347 PE LO	AY882129, AY882196, AY882259
22. Peru: Loreto; lower Rio Napo region, E bank of Rio Yanyacu, ca. 90 km N Iquitos, −3.91°, −73.08°	3	LSUMNS	4313	4313 PE LO	AY882115, AY882182, AY882245
			4410	4410 PE LO	AY882100, AY882167, AY882230
			4545[a]	2891 PE LO	AY882128, AY882195, AY882258
23. Peru: San Martin; 20 km NE Tarapoto on road to Yurimaguas, −6.41°, −75.66°	3	LSUMNS	5394	5394 PE SM	AY882093, AY882160, AY882223
			5487	5487 PE SM	AY882098, AY882165, AY882228
			5490[a]	5487 PE SM	AY882101, AY882168, AY882231
24. Peru: Loreto; 79 km WNW Contamana, −7.13°, −75.67°	3	LSUMNS	27578	27578 PE LO	AY882103, AY882170, AY882233
			27584	27584 PE LO	AY882130, AY882197, AY882260
			27832	27832 PE LO	AY882122, AY882189, AY882252
25. Peru: Ucayali; SE slope of Cerro Tahuayo, −8.13°, −74.04°	4	LSUMNS	10492	10492 PE UC	AY882078, AY882145, AY882208
			10504	10504 PE UC	AY882107, AY882174, AY882237
			11070[a]	10504 PE UC	AY882116, AY882183, AY882246
			11087[a]	10504 PE UC	AY882123, AY882190, AY882253
26. Brazil: Rondonia; ca. 50 km NW Jaciparana, w bank of Rio Maderia, −9.25°, −64.4°	1	LSUMNS	31333	31333 BR RO	AY882083, AY882150, AY882213
27. Bolivia: Pando; Nicolas Suarez, 12 km by road S Cobija, 8 km W on road to Mucden, −11.18°, −69.03°	3	LSUMNS	9125	9125 BO PA	AY882086, AY882153, AY882216
			9177[a]	9125 BO PA	AY882127, AY882194, AY882257
			9269	9269 BO PA	AY882133, AY882200, AY882263
28. Peru: Madre de Dios; Moskitania, 13.4 km NNW Atalya, L bank of the Alto Madre de Dios, −13.82°, −71.63°	6	FMNH	433689	433689 PE MD	AY882089, AY882156, AY882219
			433690	433690 PE MD	AY882104, AY882171, AY882234
			433691	433691 PE MD	AY882125, AY882192, AY882255
			433692	433692 PE MD	AY882096, AY882163, AY882226
			433693[a]	9125 BO PA	AY882111, AY882178, AY882241
			433694	433694 PE MD	AY882090, AY882157, AY882220

(*continued on next page*)

Appendix A (*continued*)

Locality	Sample size	Tissue source	Tissue number	Haplotype code	GenBank Accession Nos. (ND3, ND2, cytochrome *b*)
29. Bolivia: La Paz; Rio Beni, ca. 20 km by river N Puerto Linares, −15.5°, −67.3°	1	LSUMNS	901	901 BO LP	AY882102, AY882169, AY882232

Locality numbers correspond to Fig. 1. Haplotype codes correspond to Fig. 2, Table 3, and Supplemental Material.

Note. AMNH, American Museum of Natural History; ANSP, Academy of Natural Science—Philadelphia; FMNH, Field Museum of Natural History; KUNHM, Kansas University Natural History Museum; LSUMNS, Louisiana State University Museum of Natural Science.

[a] Individuals eliminated from tree searches because they did not carry unique haplotypes.

[b] Tissue samples from these individuals were badly decomposed making it impossible to obtain sequence data for the cytochrome *b* fragment.

Appendix B. Supplementary data

Supplementary data associated with this article can be found, in the online version, at doi:10.1016/j.ympev.2005.01.015.

References

Aleixo, A., 2002. Molecular systematics and the role of the "vàrzea"-"terra-firme" ecotone in the diversification of *Xiphorhynchus* woodcreepers (Aves: Dendrocolaptidae). Auk 119, 621–640.

Aleixo, A., 2004. Historical diversification of a *terra-firme* forest bird superspecies: a phylogeographic perspective on the role of different hypotheses of Amazonian diversification. Evolution 58, 1303–1317.

Avise, J.C., 2000. Phylogeography: The History and Formation of Species. Harvard University Press, Cambridge.

Bates, J.M., Hackett, S.J., Cracraft, J., 1998. Area-relationships in the Neotropical lowlands: a hypothesis based on raw distributions of Passerine birds. J. Biogeogr. 25, 783–793.

Bates, J.M., Hackett, S.J., Goerck, J.M., 1999. High levels of mitochondrial DNA differentiation in two lineages of Antbirds (*Drymophila* and *Hypocnemis*). Auk 116, 1039–1106.

Bates, J.M., Tello, J.G., da Silva, J.M.C., 2003. Initial assessment of genetic diversity in ten bird species of South American cerrado. Neotrop. Fauna Eviron. 38, 94–97.

Bernatchez, L., 2001. The evolutionary history of the brown trout (*Salmo trutta*) inferred from phylogeographic, nested cladistic, and mismatch analyses of mitochondrial DNA variation. Evolution 55, 351–379.

Brooks, D.R., van Veller, M.G.P., 2003. Critique of parsimony analysis of endemicity as a method of historical biogeography. J. Biogeogr. 30, 819–825.

Brumfield, R.T., Capparella, A.P., 1996. Historical diversification of birds in northwestern South America: a molecular perspective on the role of vicariant events. Evolution 50, 1607–1624.

Brumfield, R.T., Jernigan, R.W., McDonald, D.B., Braun, M.J., 2001. Evolutionary implications of divergent clines in an avian (*Manacus*:Aves) hybrid zone. Evolution 55, 2070–2087.

Bush, M.B., 1994. Amazonian speciation: a necessarily complex model. J. Biogeogr. 21, 5–17.

Bush, M.B., Colinvaux, P., Weimann, M.C., Piperno, D.R., Liu, K.-b., 1990. Late Pleistocene temperature depression and vegetational change in Ecuadorian Amazonia. Quat. Res. 34, 330–345.

Capparella, A.P., 1988. Genetic variation in neotropical birds: implications for the speciation process. Acta XIX Congr. Int. Ornithol. 19, 1658–1664.

Capparella, A.P., 1991. Neotropical avian diversity and riverine barriers. Acta XX Congr. Int. Ornithol. 20, 307–316.

Chapman, F.M., 1917. The distribution of bird-life in Colombia. Bull. Am. Mus. Nat. Hist. 36, 1–729.

Chapman, F.M., 1926. The distribution of bird-life in Ecuador. Bull. Am. Mus. Nat. Hist. 55, 1–784.

Chesser, R.T., 1999. Molecular phylogenetics of the Rhinochryptid genus *Pteroptochos*. Condor 101, 439–445.

Clement, M., Posada, D., Crandall, K.A., 2000. TCS: a computer program to estimate gene genealogies. Mol. Ecol. 9, 1657–1660.

Colinvaux, P.E., 1987. Amazon diversity in light of the paleoecological record. Q. Sci. Rev. 6, 93–114.

Colinvaux, P.E., 1993. Pleistocene biogeography and diversity in tropical forests of South America. In: Goldblatt, P. (Ed.), Biological Relationships between Africa and South America. Yale University Press, New Haven, pp. 473–499.

Colinvaux, P.E., 1998. A new vicariance model for Amazonian endemics. Global Ecol. Biogeogr. Lett. 7, 95–96.

Colinvaux, P.E., De Oliveira, P., Moreno, J.E., Miller, M.C., Bush, M.B., 1996. A long pollen record from lowland Amazonia: forest and cooling in glacial times. Science 274, 85–88.

Colinvaux, P.E., De Oliveira, P., 2000. Palaeoecology and climate of the Amazon basin during the last glacial cycle. J. Q. Sci. 15, 347–356.

Colinvaux, P.A., De Oliveira, Bush, M.B., 2000. Amazonian and neotropical plant communities on glacial time-scales: The failure of the aridity and refuge hypothesis. Quat. Sci. Rev. 19, 141–169.

Cracraft, J., Prum, R.O., 1988. Patterns and processes of diversification: speciation and historical congruence in some Neotropical birds. Evolution 42, 603–620.

de Brito, R.A., Mafrin, M.H., Sene, F.M., 2002. Nested cladistic analysis of Brazilian populations of *Drosophila serido*. Mol. Phylogenet. Evol. 22, 131–143.

Desjardins, P., Morais, R., 1990. Sequence and gene organization of the chicken mitochondrial genome: a novel gene order in higher vertebrates. J. Biol. 212, 599–634.

Durand, J.D., Templeton, A.R., Guinand, B., Imsiridou, A., Bouvet, Y., 1999. Nested clade and phylogeographic analysis of the Chub (Teleostei, Cyprinidae), in Greece: implications for Balkan Peninsula biogeography. Mol. Phylogenet. Evol. 13, 566–580.

Edwards, S.V., 1997. Relevance of microevolutionary processes to higher level systematics. In: Mindell, D.P. (Ed.), Avian Molecular Evolution and Systematics. Academic Press, San Diego, CA, pp. 251–278.

Edwards, S.V., Beerli, P., 2000. Perspective: gene divergence, population divergence, and the variance in coalescence time in phylogeographic studies. Evolution 54, 1839–1854.

Endler, J.A., 1982. Pleistocene forest refuges: fact or fancy. In: Prance, G.T. (Ed.), Biological Diversification in the Tropics. Columbia University Press, pp. 641–657.

Fleischer, R.C., McIntosh, C.E., Tarr, C.L., 1998. Evolution on a volcanic conveyor belt: using phylogeographic reconstructions and K–Ar based ages of the Hawaiian Islands to estimate molecular evolutionary rates. Mol. Ecol. 7, 533–545.

Fu, Y.-X., 1997. Statistical tests of neutrality against population growth, hitchhiking, and background selection. Genetics 147, 915–925.

Hackett, S.J., 1996. Molecular phylogenetics and biogeography of tanagers in the genus *Ramphocelus* (Aves). Mol. Phylogenet. Evol. 5, 368–382.

Hall, J.P., Harvey, D.J., 2002. The phylogeography of Amazonia revisited: new evidence from Riodinid butterflies. Evolution 56, 1489–1497.

Haffer, J., 1969. Speciation in Amazonian forest birds. Science 165, 131–137.

Haffer, J., 1970. Speciation in some Amazonian forest birds. J. Ornithol. 111, 285–331.

Haffer, J., 1974. Avian Speciation in Tropical South America. Nuttall Ornithological Club, Cambridge.

Haffer, J., 1990. Avian species richness in tropical South America. Neotrop. Fauna Environ. 25, 157–183.

Haffer, J., 1997. Alternative models of vertebrate speciation in Amazonia: an overview. Biodiv. Cons. 6, 451–476.

Harpending, H., 1994. Signature of ancient population growth in a low resolution mitochondrial mismatch distribution. Hum. Biol. 66, 131–137.

Hasegawa, M., Kishino, K., Yano, T., 1985. Dating the human–ape splitting by a molecular clock of mitochondrial DNA. J. Mol. Evol. 22, 160–174.

Hewitt, G., 1996. Some genetic consequences of ice ages, and their role in divergence and speciation. Biol. J. Linn. Soc. 58, 247–276.

Hewitt, G., 2000. The genetic legacy of the Quaternary ice ages. Nature 405, 907–913.

Hoffman, E.A., Blouin, M.S., 2004. Evolutionary history of the northern Leopard Frog: reconstruction of phylogeny, phylogeography, and historical changes in population demography from mitochondrial DNA. Evolution 58, 145–159.

Hoffman, F.G., Baker, R.G., 2003. Comparative phylogeography of short-tailed bats (*Carollia*: Phyllostomidae). Mol. Ecol. 12, 3403–3414.

Hooghiemstra, H., van der Hammen, T., 1998. Neogene and Quaternary development of the neotropical rainforest: the forest refugia hypothesis and a literature review. Earth Sci. Rev. 44, 147–183.

Hulsenbeck, J.P., Ronquist, F., 2001. MRBAYES: Bayesian inference of phylogeny. Bioinformatics 17, 754–755.

Joseph, L., Wilke, T., Alpers, D., 2002. Reconciling genetic expectations from host specificity with historical population dynamics in an avian brood parasite, Horsfield's Bronze Cuckoo *Chalcites basalis* of Australia. Mol. Ecol. 11, 829–837.

Knowles, L.L., Maddison, W.P., 2002. Statistical phylogeography. Mol. Ecol. 11, 2623–2635.

Kocher, T.D., Wilson, W.K., Meyer, A., Edwards, S.V., Pääbo, S., Villablanca, F.X., Wilson, A.K., 1989. Dynamics of mitochondrial DNA evolution in animals: amplification and sequencing with conserved primers. Proc. Natl. Acad. Sci. USA 86, 6196–6200.

Lessa, E.P., Cook, J.A., Patton, J.L., 2003. Genetic footprints of demographic expansion in North America, but not Amazonia, during the late Quaternary. Proc. Natl. Acad. Sci. USA 100, 10331–10334.

Liu, K.-B., Colinvaux, P.E., 1985. A 5200-year history of the Amazon rain forest. J. Biogeogr. 15, 231–248.

Marks, B.D., Hackett, S.J., Capparella, A.P., 2002. Historical relationships among Neotropical lowland forest areas of endemism as inferred from mitochondrial DNA sequence variation within the Wedge-billed Woodcreeper (Aves: Dendrocolaptidae: *Glyphorynchus spirurus*). Mol. Phylogenet. Evol. 24, 155–167.

Masta, S.M., Laurent, N.M., Routman, E.J., 2003. Population genetic structure of the toad *Bufo woodhousii*: an empirical assessment of the effects of haplotype extinction on nested cladistic analyses. Mol. Ecol. 12, 1541–1554.

Moritz, C., Patton, J.L., Schneider, C.J., Smith, T.B., 2000. Diversification of rainforest faunas: an integrated molecular approach. Annu. Rev. Ecol. Syst. 31, 533–563.

Nei, M., 1987. Molecular Evolutionary Genetics. Columbia University Press, New York.

Nesbo, C.L., Fossheim, T., Vøllestad, L.A., Jackobsen, K.S., 1999. Genetic divergence and phylogeographic relationships reflect glacial refugia and postglacial colonization. Mol. Ecol. 8, 1387–1404.

Nores, M., 1999. An alternative hypothesis for the origin of Amazonian bird diversity. J. Biogeogr. 26, 475–485.

Paetkau, D., Shields, G.F., Strobeck, C., 1998. Gene flow between insular, coastal and interior populations of brown bears in Alaska. Mol. Ecol. 7, 1283–1292.

Pavlova, A., Zink, R.M., Drovetski, S.V., Red'kin, Y., Rohwer, S., 2003. Phylogeographic patterns in Motacilla flava and Motacilla citreola: species limits and population history. Auk 120, 744–758.

Posada, D., Crandall, K.A., 1998. Modeltest: testing the model of DNA substitution. Bioinformatics 14, 817–818.

Posada, D., Crandall, K.A., Templeton, A.R., 2000. GeoDis: a program for the cladistic nested analysis of the geographical distribution of genetic haplotypes. Mol. Ecol. 9, 487–488.

Prum, R.O., 1988. Historical relationships among avian forest areas of endemism in the Neotropics. Acta XIX Congr. Int. Ornithol. 19, 2562–2572.

Rasanen, M.E., Linna, A.M., Santos, J.C.R., Negri, F.R., 1995. Late Miocene tidal deposits in the Amazonian foreland basin. Science 269, 386–390.

Ridgley, R., Tudor, G., 1994. The Birds of South America Volume II: The Suboscine Passerines. University of Texas Press, Austin.

Rogers, A.R., 1995. Genetic evidence for a Pleistocene population explosion. Evolution 4, 608–615.

Romis-Onsins, S.E., Rozas, J., 2002. Statistical properties of new neutrality tests against population growth. Mol. Biol. Evol. 19, 2092–2100.

Rozas, J., Rozas, R., 1999. DnaSp version 3: an integrated program for molecular population genetics and molecular evolution analysis. Bioinformatics 15, 174–175.

Schneider, S., Roessli, D., Excoffier, L., 2000. Arlequin, version 2.0: a software for genetic data analysis. Genetics and Biometry Laboratory, Geneva.

Sgariglia, E.A., Burns, K.J., 2003. Phylogeography of the California Thrasher (Toxostoma redivivum) based on nested-clade analysis of mitochondrial-DNA variation. Auk 120, 346–363.

Sick, H., 1967. Rios e enchentes na Amazonia como obstaculo para a avifauna. In: H. Lent (Ed.). Atas do simposio sobre a biota amazonica, vol. 5 (Zoologia). Conselho de Pesquisas Rio de Janeiro, pp. 495–520.

Snow, D., 2004. Family Pipridae (Manakins). In: del Hoyo, J., Elliot, A., Christie, D. (Eds.). Handbook of Birds of the World, vol. 9. Lynx Edicions, Barcelona, pp. 110–169.

Sorenson, M.D., Quinn, T.W., 1998. Numts: a challenge for avian systematics and population biology. Auk 115, 214–221.

Swofford, D.L., 1999. PAUP*. Phylogenetic analysis using parsimony (* and other methods). Version 4.0b10. Sinauer Associates, Sunderland, Massachusetts.

Templeton, A.R., 1998. Nested clade analyses of phylogeographic data: testing hypotheses about gene flow and population history. Mol. Ecol. 7, 381–397.

Templeton, A.R., 2004. Statistical phylogeography: methods for evaluating and minimizing inference errors. Mol. Ecol. 13, 789–809.

Templeton, A.R., Crandall, K.A., Sing, C.F., 1992. A cladistic analysis of phenotypic associations with haplotypes inferred from restriction endonuclease mapping and DNA sequence data III: cladogram estimation. Genetics 132, 619–633.

Templeton, A.R., Sing, C.F., 1993. A cladistic analysis of phenotypic associations with haplotypes inferred from restriction endonuclease mapping IV: nested analysis with cladogram uncertainty and recombination. Genetics 134, 659–669.

Templeton, A.R., Boerwinkle, E., Sing, C.F., 1987. A cladistic analysis of phenotypic associations with haplotypes inferred from restriction endonuclease mapping I: Basic theory and an analysis of alcohol dehydrogenase activity in Drosophila. Genetics 117, 343–351.

Templeton, A.R., Routman, E., Phillips, C., 1995. Separating population structure from population history: a cladistic analysis of the geographical distribution of mtDNA haplotypes in the Tiger Salamander, *Ambystoma tigrinum*. Genetics 140, 767–782.

Todd, W.E., 1925. Sixteen new birds from Brazil and Guiana. Proc. Biol. Soc. Wash. 38, 90–99.

Traylor Jr., M.A., 1979. Checklist of the Birds of the World: A Continuation of the Work of James Peters, vol. VIII. Museum of Comparative Zoology, Cambridge.

Voelker, G., 1999. Dispersal, vicariance, and clocks: historical biogeography and speciation in a cosmopolitan passerine genus (*Anthus*: Motacillidae). Evolution 53, 1536–1552.

Wallace, A.R., 1889. Travels on the Amazon. Harper and Row, New York.

Webb, S.D., 1995. Biological implications of the Middle Miocene Amazon seaway. Science 269, 361–362.

Wilke, T., Pfenniger, M., 2002. Separating historic events from the recurrent processes in cryptic species: phylogeography of mud snails (*Hydrobia* spp.). Mol. Ecol. 11, 1439–1451.

Zheng, X., Arbogast, B.S., Kenagy, G.J., 2003. Historical demography and genetic structure of sister species: deermice (*Peromyscus*) in the North American temperate rain forest. Mol. Ecol. 12, 711–724.

Zink, R.M., 2004. The role of subspecies in obscuring avian biological diversity and misleading conservation policy. Proc. R. Soc. Lond. B 271, 561–564.

Zink, R.M., Barrowclough, G.F., Atwood, J.L., Blackwell-Rago, R.C., 2000. Genetics, taxonomy, and conservation of the threatened California Gnatcatcher. Cons. Biol. 14, 1394–1405.